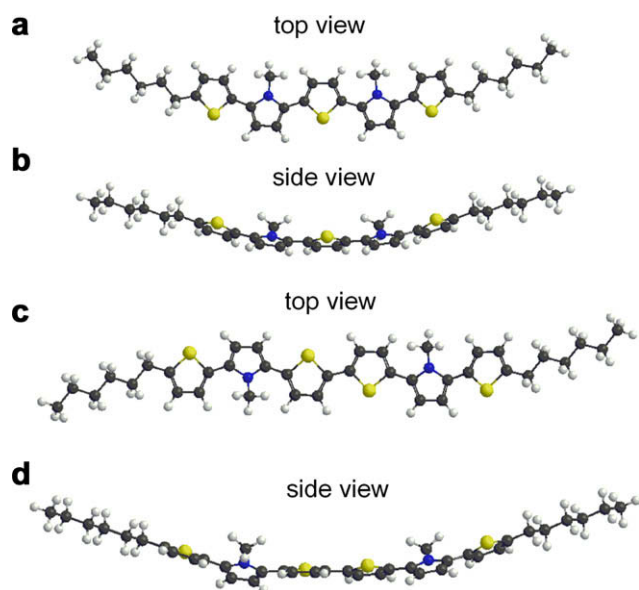




First we attempted to synthesize **1** (R = H), but we failed to obtain the product pure enough for FET application due to the instability of the products. Thus, **1** (R = Me) were synthesized from **5**. Similarly, the synthesis of hexamer **2** (R = Me) was conducted by Paal–Knorr reaction of asymmetric diketone **6** followed by homo-coupling of the resultant trimer. For the synthesis of the precursors of asymmetric 1,4-diketones **5** and **6**, we chose cross-coupling of methyl ketone and  $\alpha$ -bromomethyl ketone in the presence of  $\text{ZnCl}_2$ -*t*-BuOH- $\text{Et}_2\text{NH}$ <sup>11</sup> instead of Stetter's procedure.<sup>9f</sup> The advantages of the former method are the facile access to the precursors and avoiding the use of toxic sodium cyanide.

These oligomers **1** (R = Me) and **2** (R = Me) are yellow and orange crystals, respectively, soluble in common organic solvents, and stable in the solid and solution phases. Thus, they can be purified by normal recrystallization from dichloromethane–hexane, even though the solubility of **2** (R = Me) (ca. 2 mg/ml in  $\text{CH}_2\text{Cl}_2$ ) is less than that of **1** (R = Me) (ca. 20 mg/ml in  $\text{CH}_2\text{Cl}_2$ ). The moderate solubility of **2** (R = Me) is in contrast to the case of longer **DH-SOSOSOS** heptamer (ca. 10 mg/ml in  $\text{CH}_2\text{Cl}_2$ ),<sup>7a</sup> and can be rationalized by the difference in the molecular structures as described below.

We tried to obtain single crystals suitable for X-ray structural analysis, but all attempts have not succeeded so far. Thus, the structures of **1** (R = Me) and **2** (R = Me) were estimated by DFT calculations at the B3LYP/6-31G(d) level (see [Supplementary data](#) for details). As shown in [Figure 1](#), the thiophene and pyrrole rings are twisted from coplanarity for both cases due to the presence of the steric repulsion between methyl group and the adjacent thiophene rings. The averaged dihedral angles at S–C–C–N connections are 147° for both cases. As concerns the molecular shapes, a top view of **1** (R = Me) shows a banana-shaped structure. This deformation takes place because of the difference in the bond angles of S–C–C and N–C–C connections between thiophene and pyrrole rings which stems from the different lengths between the S–C and N–C bonds. Similar deformations were also observed in the alternately connected thiophene–furan oligomers.<sup>7a</sup> On the other hand, a top view of **2** (R = Me) shows a nearly linear structure with a gentle S-shape, though the side views of both oligomers show bent structures. These bending structures on the side views may be flattened by packing force in solid states, but the flattening of the  $\pi$ -systems essentially does not alter the shape on the top



**Figure 1.** Top and side views of the optimized structures of (a) **1** (R = Me) and (c) **2** (R = Me).

**Table 1**

Absorption maxima and oxidation potentials of the oligomers

Compd	Abs <sub>max</sub> (nm)	$E_{1/2}^{\text{ox1a}}$ (V)	$E_{1/2}^{\text{ox2a}}$ (V)
<b>1</b> (R = Me)	370 <sup>b</sup>	0.06 <sup>c,d</sup>	0.20
<b>DH-SOSOS</b>	421 <sup>e,f</sup>	0.20 <sup>c,f,g</sup>	0.51
<b>DH-SSSSS</b>	426 <sup>e,h</sup>	0.37 <sup>d,e,h</sup>	0.59
<b>2</b> (R = Me)	405 <sup>b</sup>	0.08 <sup>c,d</sup>	0.16
<b>DH-SSSSSS</b>	440 <sup>e,h</sup>	0.33 <sup>d,e,h</sup>	0.55

<sup>a</sup> V versus Fc/Fc<sup>+</sup>.

<sup>b</sup> In benzene.

<sup>c</sup> In dichloromethane.

<sup>d</sup> 0.1 M *n*-Bu<sub>4</sub>NPF<sub>6</sub>.

<sup>e</sup> In THF.

<sup>f</sup> Ref. 7a.

<sup>g</sup> 0.1 M *n*-Bu<sub>4</sub>NClO<sub>4</sub>.

<sup>h</sup> Ref. 12.

views. Thus, the linearity of **2** (R = Me) may cause greater van der Waals contact in solid states and hence decrease the solubility.

The electronic absorption maxima and oxidation potentials of **1** (R = Me) and **2** (R = Me) are summarized in [Table 1](#), together with the data of the corresponding dihexyl-oligothiophenes (**DH-SSSSS**, **DH-SSSSSS**)<sup>12</sup> and mixed pentamer (**DH-SOSOS**).<sup>7a</sup> The absorption maxima of **1** (R = Me) and **2** (R = Me) show a large hypsochromic shift due to the out-of-plane distortion of the  $\pi$ -system as predicted by the DFT calculations. Nevertheless, the oxidation potentials of **1** (R = Me) and **2** (R = Me) are much lower than those of **DH-SSSSS**, **DH-SSSSSS**, and **DH-SOSOS** owing to the presence of the electron-rich pyrrole moiety. This idea is consistent with the fact that the  $\pi$ -extension by the insertion of one thiophene ring from **1** (R = Me) to **2** (R = Me) does not affect much the oxidation potentials.

The FET devices of **1** (R = Me) and **2** (R = Me) were fabricated by vacuum deposition of the oligomers on bare or octadecyltrichlorosilane (OTS) treated Si/SiO<sub>2</sub> substrates and then source and drain Au

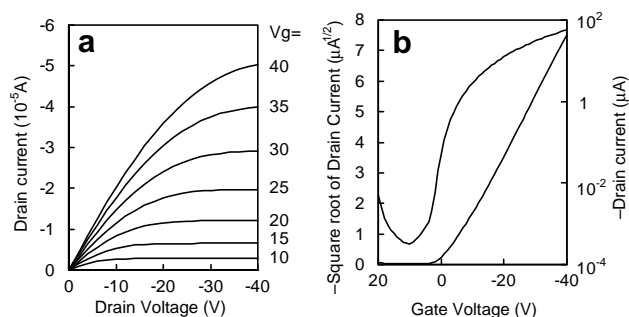


**Figure 2.** (a) Output characteristic and (b) transfer characteristic at –40 V of drain voltage for **2** (R = Me) with OTS treatment. Gate dielectric layer is a thermally oxidized 200 nm thick SiO<sub>2</sub> and the channel length and width are 0.05 and 5 mm, respectively.

**Table 2**

Field-effect characteristics of the oligomers

Compd	SiO <sub>2</sub> treatment	$\mu$ (cm <sup>2</sup> V <sup>-1</sup> s <sup>-1</sup> )	$I_{\text{on}}/I_{\text{off}}$	$V_{\text{th}}$ (V)
<b>1</b> (R = Me)	Bare	$7.9 \times 10^{-3}$	10 <sup>3</sup>	17
<b>1</b> (R = Me)	OTS	$9.1 \times 10^{-3}$	10 <sup>4</sup>	–5.4
<b>DH-SOSOS</b> <sup>a</sup>	OTS	$3.6 \times 10^{-2}$	10 <sup>3</sup>	–2
<b>DH-SSSSS</b> <sup>b</sup>	Bare	$5.1 \times 10^{-2}$	10 <sup>4</sup>	–1
<b>2</b> (R = Me)	Bare	$1.2 \times 10^{-2}$	10 <sup>4</sup>	–1
<b>2</b> (R = Me)	OTS	$5.3 \times 10^{-2}$	10 <sup>5</sup>	–2.3
<b>DH-SSSSSS</b> <sup>b</sup>	Bare	$4.4 \times 10^{-2}$	$2 \times 10^3$	–2

<sup>a</sup> Ref. 7a.

<sup>b</sup> Ref. 4f.

electrodes with top-contact configuration.<sup>13</sup> The measurements were conducted under air. As shown in Figure 2 and Table 2, these oligomers behave as p-type semiconductors. In spite of the distorted structure in solution, **1**(R = Me) showed good hole mobility ( $\mu = 9.1 \times 10^{-3} \text{ cm}^2 \text{ V}^{-1} \text{ s}^{-1}$  with OTS treatment), which is comparable to those of more planar **DH-SSSSS** and **DH-SOSOS**. Furthermore, **2**(R = Me) with nearly linear structure exhibited better FET

**Table 3**  
Observed *d*-spacings and molecular lengths for films of the oligomers

Compd	<i>d</i> Spacing (nm)	Molecular length (nm)
<b>1</b> (R = Me)	—	3.3 <sup>a</sup>
<b>DH-SOSOS</b> <sup>b</sup>	3.06	3.15 <sup>c</sup>
<b>DH-SSSSS</b> <sup>d</sup>	3.0	3.74 <sup>c,e</sup>
<b>2</b> (R = Me)	3.15	3.7 <sup>a</sup>
<b>DH-SSSSS</b> <sup>d</sup>	3.54	3.92 <sup>c,e</sup>

<sup>a</sup> Estimated by DFT calculations.

<sup>b</sup> Ref. 7a.

<sup>c</sup> Determined by X-ray analysis.

<sup>d</sup> Ref. 4f.

<sup>e</sup> Both lengths include standard van der Waals radii for carbon (1.70 Å) or hydrogen atoms (1.20 Å).

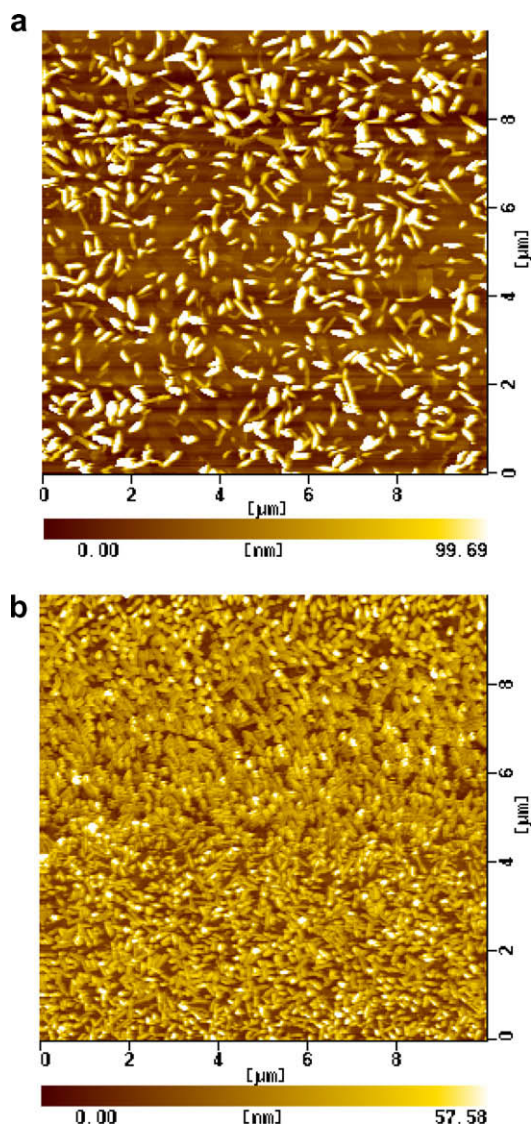


**Figure 3.** AFM images of thin films of (a) **1**(R = Me) and (b) **2**(R = Me) with OTS treatment.

characteristics ( $\mu = 5.3 \times 10^{-2} \text{ cm}^2 \text{ V}^{-1} \text{ s}^{-1}$ ,  $I_{\text{on}}/I_{\text{off}} = 10^5$ , and  $V_{\text{th}} = -2.3 \text{ V}$  with OTS treatment) than those of **1**(R = Me) with a banana-shaped structure, suggesting that the enhanced molecular linearity causes the better FET performance.

To investigate the thin film structures, the XRD measurements were performed. As shown in Table 3 and Figure S21, the overall structure of the film of **2**(R = Me) is layered with the *d*-spacing obtained from the first reflection peak being 3.15 nm. Since the molecular length estimated by the DFT calculations (**2**(R = Me) 3.7 nm) is slightly larger than the *d*-spacing value, the molecule is slightly tilted from a vertical orientation to the substrate. The tilt angle is similar to those of oligothiophenes, although these angles can not be directly compared due to the difference in the estimation method of the molecular length. In contrast, the XRD pattern of the film of **1**(R = Me) (Fig. S20) appears to be assigned to microcrystalline phase. Thus, the films were also investigated by atomic force microscope (AFM) to compare the film morphologies of **1**(R = Me) and **2**(R = Me). As shown in Figure 3, many small grains with similar size were observed in both films but the grains of **2**(R = Me) appeared to be denser, which is considered to cause the better FET performance of **2**(R = Me).

In summary, we have newly synthesized thiophene–methylpyrrole mixed oligomers **1**(R = Me) and **2**(R = Me), and revealed for the first time that this type of oligomers showed p-type FET behavior as good as the corresponding oligothiophenes. In comparison between **1**(R = Me) and **2**(R = Me), the  $\pi$ -extension by the incorporation of one thiophene ring does not affect the HOMO levels. However, the hole mobility of **2**(R = Me) is significantly enhanced due to the nearly linear molecular structure of **2**(R = Me) which seems to cause the greater intermolecular interaction and better film morphology.

### Acknowledgments

This work was supported by Grant-in-Aid for Scientific Research (C) (No. 19550049) from the Ministry of Education, Culture, Sports, Science and Technology of Japan. We thank Mr. Katsura Hirai and Mr. Tatsuya Tanaka (Konica Minolta Technology Center, Inc.) for preparation of thin films and measurements of field-effect properties, AFM, and XRD of these films.

### Supplementary data

Supplementary data associated with this article can be found, in the online version, at doi:10.1016/j.tetlet.2008.11.061.

### References and notes

- For recent reviews see: (a) Allard, S.; Forster, M.; Souharce, B.; Thiem, H.; Scher, U. *Angew. Chem., Int. Ed.* **2008**, *47*, 4070; (b) Zaumseil, J.; Sirringhaus, H. *Chem. Rev.* **2007**, *107*, 1296; (c) Murphy, A. R.; Fréchet, J. M. J. *Chem. Rev.* **2007**, *107*, 1066.
- Forrest, S. R. *Nature* **2004**, *428*, 911.
- (a) Yamamoto, T.; Takimiya, K. *J. Am. Chem. Soc.* **2007**, *129*, 2224; (b) Mamada, M.; Nishida, J.-i.; Kumaki, D.; Tokito, S.; Yamashita, Y. *Chem. Mater.* **2007**, *19*, 5404; (c) Takimiya, K.; Ebata, H.; Sakamoto, K.; Izawa, T.; Otsubo, T.; Kunugi, Y. *J. Am. Chem. Soc.* **2006**, *128*, 12604; (d) Naraso; Nishida, J.; Kumaki, D.; Tokito, S.; Yamashita, Y. *J. Am. Chem. Soc.* **2006**, *128*, 9598; (e) Meng, H.; Sun, F.; Goldfinger, M. B.; Gao, F.; Londono, D. J.; Marshal, W. J.; Blackman, G. S.; Dobbs, K. D.; Keys, D. E. *J. Am. Chem. Soc.* **2006**, *128*, 9304; (f) Roy, V. A. L.; Zhi, Y. G.; Xu, Z. X.; Yu, S. C.; Chan, P. W. H.; Che, C. M. *Adv. Mater.* **2005**, *17*, 1258; (g) Payne, M. M.; Parkin, S. R.; Anthony, J. E.; Kuo, C. C.; Jackson, T. N. *J. Am. Chem. Soc.* **2005**, *127*, 4986; (h) Meng, H.; Sun, F.; Goldfinger, M. B.; Jaycox, G. D.; Li, Z.; Marshall, W. J.; Blackman, G. S. *J. Am. Chem. Soc.* **2005**, *127*, 2406.
- (a) Ie, Y.; Umamoto, Y.; Okabe, M.; Kusuniki, T.; Nakayama, K.; Pu, Y.-J.; Kido, J.; Tada, H.; Aso, Y. *Org. Lett.* **2008**, *10*, 833; (b) Yoon, M.-H.; Facchetti, A.; Stern, C. E.; Marks, T. J. *J. Am. Chem. Soc.* **2006**, *128*, 5792; (c) Zen, A.; Bilge, A.; Galbrecht, F.; Alle, R.; Meerholz, K.; Grenzer, J.; Neher, D.; Scherf, U.; Farrell, T. *J. Am. Chem. Soc.* **2006**, *128*, 3914; (d) Yoon, M. H.; DiBenedetto, S. A.; Facchetti, A.; Marks, T. J. *J. Am. Chem. Soc.* **2005**, *127*, 1348; (e) Nagamatsu, S.; Kaneto, K.; Azumi, R.; Matsumoto, M.; Yoshida, Y.; Yase, K. *J. Phys. Chem. B* **2005**, *109*, 9374; (f)

- Facchetti, A.; Mushrush, M.; Yoon, M. H.; Hutchison, G. R.; Ratner, M. A.; Marks, T. J. *J. Am. Chem. Soc.* **2004**, *126*, 13859; (g) Murphy, A. R.; Frechet, J. M. J.; Chang, P.; Lee, J.; Subramanian, V. *J. Am. Chem. Soc.* **2004**, *126*, 1596; (h) Kunugi, Y.; Takimiya, K.; Yamane, K.; Yamashita, K.; Aso, Y.; Otsubo, T. *Chem. Mater.* **2003**, *15*, 6; (i) Halik, M.; Klauk, H.; Zschieschang, U.; Schmid, G.; Radlik, W.; Ponomarenko, S.; Kirchmeyer, S.; Weber, W. *Adv. Mater.* **2003**, *15*, 917.
- Miyata, Y.; Nishinaga, T.; Komatsu, K. *J. Org. Chem.* **2005**, *70*, 1147.
  - Cornil, J.; Beljonne, D.; Calbert, J.-P.; Brédas, J. L. *Adv. Mater.* **2001**, *13*, 1053.
  - (a) Miyata, Y.; Terayama, M.; Minari, T.; Nishinaga, T.; Nemoto, T.; Isoda, S.; Komatsu, K. *Chem. Asian J.* **2007**, *2*, 1492; (b) Minari, T.; Miyata, Y.; Terayama, M.; Nemoto, T.; Nishinaga, T.; Komatsu, K.; Isoda, S. *Appl. Phys. Lett.* **2006**, *88*, 083514.
  - Sessler, J. L.; Aguilar, A.; Sanchez-Garcia, D.; Seidel, D.; Kohler, T.; Arp, F.; Lynch, V. M. *Org. Lett.* **2005**, *7*, 1887.
  - (a) Ogura, K.; Yanai, H.; Miokawa, M.; Akazome, M. *Tetrahedron Lett.* **1999**, *40*, 8887; (b) van Haare, J. A. E. H.; Groenendaal, L.; Havinga, E. E.; Meijer, E. W.; Janssen, R. A. J. *Synth. Met.* **1997**, *85*, 1091; (c) Groenendaal, L.; Peerlings, H. W. I.; Havinga, E. E.; Vekemans, J. A. J. M.; Meijer, E. W. *Synth. Met.* **1995**, *69*, 467; (d) Parakka, J. P.; Cava, M. P. *Synth. Met.* **1995**, *68*, 275; (e) Niziurski-Mann, R. E.; Cava, M. P. *Adv. Mater.* **1993**, *5*, 547; (f) Stetter, H. *Angew. Chem., Int. Ed. Engl.* **1976**, *15*, 639.
  - Hoppe, A.; Seekamp, J.; Balster, T.; Götz, G.; Bäuerle, P.; Wagner, V. *Appl. Phys. Lett.* **2007**, *91*, 132115.
  - Nevar, N. M.; Kel'in, A. V.; Kulinkovich, O. G. *Synthesis* **2000**, 1259.
  - Facchetti, A.; Yoon, M.-H.; Stern, C. L.; Hutchison, G. R.; Ratner, M. A.; Marks, T. J. *J. Am. Chem. Soc.* **2004**, *126*, 13480.
  - See [Supplementary data](#) for detailed experimental conditions.